available at www.sciencedirect.com

ScienceDirect

journal homepage: www.elsevier.com/locate/biochempharm

Circumvention and reactivation of the p53 oncogene checkpoint in mouse colon tumors

Wataru Aizu [a], *Glenn S. Belinsky* [b], *Christopher Flynn* [b], *Emily J. Noonan* [a], *Colleen C. Boes* [a], *Cassandra A. Godman* [a], *Bindi Doshi* [a], *Prashant R. Nambiar* [b,1], *Daniel W. Rosenberg* [b], *Charles Giardina* [a,*]

[a] *Department of Molecular & Cell Biology, 91 North Eagleville Road, University of Connecticut, Storrs, CT 06269-3125, USA*
[b] *Center for Molecular Medicine, University of Connecticut Health Center, Farmington, CT 06030, USA*

ARTICLE INFO

Article history:
Received 29 March 2006
Accepted 17 July 2006

Keywords:
Colon cancer
p19/ARF
p53
Mdm2
Nutlin-3
Azoxymethane
Mouse model

ABSTRACT

The p53 tumor suppressor protein is sequence-normal in azoxymethane (AOM)-induced mouse colon tumors, making them a good model for human colon cancers that retain a wild type p53 gene. Cellular localization and co-immunoprecipitation experiments using a cell line derived from an AOM-induced colon tumor (AJ02-NM_0 cells) pointed to constitutively expressed Mdm2 as being an important negative regulator of p53 in these cells. Although the Mdm2 inhibitory protein p19/ARF was expressed in AJ02-NM_0 cells, its level of expression was not sufficient for p53 activation. We tested the response of AJ02-NM_0 cells to the recently developed Mdm2 inhibitor, Nutlin-3. Nutlin-3 was found to activate p53 DNA binding in AJ02-NM_0 cells, to a level comparable to doxorubicin and 5-fluorouracil (5-FU). In addition, Nutlin-3 increased expression of the p53 target genes Bax and PERP to a greater extent than doxorubicin or 5-FU, and triggered a G2/M phase arrest in these cells, compared to a G1 arrest triggered by doxorubicin and 5-FU. The differences in the cellular response may be related to differences in the kinetics of p53 activation and/or its post-translational modification status. In an ex vivo experiment, Nutlin-3 was found to activate p53 target gene expression and apoptosis in AOM-induced tumor tissue, but not in normal adjacent mucosa. Our data indicate that Mdm2 inhibitors may be an effective means of selectively targeting colon cancers that retain a sequence-normal p53 gene while sparing normal tissue and that the AOM model is an appropriate model for the preclinical development of these drugs.

1. Introduction

The p19/ARF-p53 oncogene checkpoint plays a critical role in suppressing carcinogenesis [1]. This checkpoint is mobilized through the oncogene-induced activation of p19/ARF expression, which then signals p53 activation. p19/ARF activates p53 by localizing the Mdm2 inhibitory protein to the nucleolus away from p53 [2,3], or by forming a ternary complex with p53 and Mdm2 in a manner that suppresses p53 ubiquitination by Mdm2 [4,5]. Cancer development often requires an inhibition of some component of the p19/ARF-p53 tumor suppressor pathway. Although this inhibition is sometimes achieved through genetic or epigenetic mechanisms, reversible inhibitory mechanisms have also been described. A better

* *Corresponding author*. Tel.: +1 860 486 0089; fax: +1 860 486 4331.
E-mail address: charles.giardina@uconn.edu (C. Giardina).
[1] Present address: Department of Pathology, Genzyme Corporation, One Mountain Road, P.O. Box 9322, Framingham, MA 01701-9322, USA.

0006-2952/$ – see front matter
doi:10.1016/j.bcp.2006.07.009

understanding of how the p19/ARF-p53 oncogene checkpoint is inhibited in neoplasms could suggest ways to selectively stimulate this pathway in tumors where it is genetically intact yet functionally inactive.

Cancer cells can evolve a number of mechanisms to suppress the actions of a sequence-normal p53 gene. In some instances, the p53 protein can be induced to fold into an inactive conformation. For example, electrophilic agents including certain prostaglandins have been shown to inactivate thioredoxin reductase, which in turn leads to p53 oxidation and misfolding [6,7]. A number of cancer-related proteins have also been found to inactivate p53 by sequestering it within the cytoplasm. For example, Parc (p53-associated, Parkin-like cytoplasmic protein) anchors p53 protein in the cytoplasm of neuroblastoma cells [8–10]. The Hsp70 family member protein Mot-2 also directly binds to p53 and sequesters it into the cytoplasm, where it can associate with the mitochondria [11–13]. Perhaps the most common mechanism by which p53 activity is suppressed in tumors is through amplification of the Mdm2 gene, which occurs in approximately 7% of all cancers [14,15]. Increased expression of this protein can promote the ubiquitin-dependent proteasome degradation of p53, or prevent p53 from interacting with transcriptional regulatory proteins [16,17]. In either instance, the tumor-suppressing function of p53 is abrogated.

Colon tumors induced in mice by azoxymethane (AOM) activate p19/ARF expression and stabilize the p53 protein to some extent. Despite detectable p53 protein expression in these tumors, p53 DNA binding and transcriptional activation is still lacking [18]. Here, we obtain evidence that p53 in AOM-induced tumors is inhibited by its stable association with Mdm2 and that p53 function can be re-activated by treatment of these cells with the specific Mdm2 inhibitor, Nutlin-3 [19]. These studies underscore the potential therapeutic application of Mdm2 inhibitors for the treatment of colon tumors in which Mdm2 is limiting activity of the p53 protein and indicate that the AOM model is particularly well suited for the pre-clinical evaluation of these agents.

2. Materials and methods

2.1. Cell culture and treatments

AJ02-NM_0 cells were cultured in RPMI 1640 with Glutamax (Invitrogen, Carlsbad, CA) supplemented with 5% fetal bovine serum, 5% heat-inactivated horse serum, 1% insulin-transferrin-selenium-linoleic acid (Cambrex, East Rutherford, NJ), 100 μM non-essential amino acids (Invitrogen) and antibiotic–antimycotic (Invitrogen) [20]. Doxorubicin and 5-fluorouracil (5-FU) were purchased from Sigma (St. Louis, MO) and used at a final concentration of 500 nM and 100 μM, respectively. The Mdm2 inhibitor Nutlin-3 was purchased from Cayman Chemical (Ann Arbor, MI).

2.2. Cell fractionation

AJ02-NM_0 cells were washed twice with cold PBS buffer and incubated in lysis buffer A (10 mM Hepes, pH 7.6, 15 mM KCl and 2 mM $MgCl_2$ plus 0.1% Nonidet P-40) supplemented with proteinase inhibitor/phosphatase inhibitor cocktails (Sigma) and 1 mM DTT for 8 min on ice. The cells were then scraped into tubes and centrifuged for 10 min at 4 °C (14,000 rpm). The resulting supernatant was the cytoplasmic extract. The resulting nuclear pellets were rinsed with the above buffer A without NP-40. Nuclear extracts were prepared by resuspending nuclear pellets with a high-salt buffer C (20 mM Hepes, pH 7.6, 1.5 mM $MgCl_2$, 420 mM NaCl, 0.2 mM EDTA, 1 mM DTT, 5% glycerol and proteinase/phosphatase inhibitor cocktails), incubating on ice for 40 min and then centrifuging for 10 min at 4 °C (14,000 rpm). The nuclear matrix-associated fraction (including the nucleolus) was recovered by sonicating the resulting pellet in 30 μl (35 mm dish) of a 1% SDS solution. For DNA binding assays (EMSA) and immunoprecipitation assays, the salt concentration of the nuclear extracts was adjusted by mixing with a low-salt buffer D (20 mM Hepes, pH 7.6, 50 mM KCl, 0.2 mM EDTA, 1 mM DTT, 20% glycerol and proteinase/phosphatase inhibitor cocktails). Protein concentrations of the nuclear and cytoplasmic extracts were determined by the Bradford assay (Bio-Rad Laboratories, Hercules, CA), and the extracts were stored at −80 °C until they were used.

2.3. Immunoblotting and immunofluorescence

For immunoblotting studies, 10 μg of cytoplasmic, nuclear protein (quantified by the Bio-Rad protein assay) or 10 μl of matrix-associated fraction was denatured under reducing conditions, separated on 10% SDS-polyacrylamide gels and transferred to nitrocellulose by voltage gradient transfer. The resulting blots were blocked with 5% non-fat dry milk in PBS + 1% Tween. Specific proteins were detected with appropriate antibodies using enhanced chemiluminescence detection (Santa Cruz Biotechnology, Santa Cruz, CA) as recommended by the manufacturer. Immunoblotting antibodies against p19/ARF (G-19), nucleolin (MS-3) and actin (I-19) were obtained from Santa Cruz Biotechnology and antibodies against p53 (Ab-1) and Mdm2 (Ab-2) were obtained from Oncogene Research Products (San Diego, CA). For immunofluorescence, AJ02-NM_0 cells were washed with cold phosphate-buffered saline and fixed with 100% methanol for 30 min at −20 °C. The methanol was removed, and permeabilizing reagent (0.5% Triton X-100) was added to the cells for 15 min at 4 °C. Cells were then incubated in 5% normal-control serum for 30 min, to block non-specific antibody binding. After blocking, the cells were incubated with primary antibody at a 1:100 dilution followed by incubation with fluorescein-conjugated or Texas red-conjugated secondary antibody (Jackson ImmunoResearch Laboratories, West Grove, PA). Fluorescent imaging was performed on an inverted microscope (Eclipse TE 300; Nikon, Melville, NY, USA) using a 20× objective. Images were acquired using a CCD camera (Quantix 57, Roper Scientific, Tuscon, AZ). Antibodies used for immunofluorescence were a rabbit polyclonal ARF antibody (Novus Biologicals, Littleton, CO), a rabbit polyclonal p53 CM5 antibody (Novacastra, Newcastle upon Tyne, UK) and a mouse monoclonal Mdm2 antibody (Ab-2, Oncogene Research Products).

2.4. Immunoprecipitation

Nuclear protein extract (80 μg for each sample) was precleared with protein A-Sepharose (Amersham Biosciences, Piscataway, NJ). Five microliters of a p53 mouse monoclonal antibody (Ab-1, Oncogene Research Products) was then added to each sample and incubated at 4 °C overnight with gentle rocking. Precipitation was performed by incubating extracts with 10 μl of protein A-Sepharose for 2 h at 4 °C, centrifuging for 1 min at 12,000 × *g* and then washing the pellet with ice-cold TNT Buffer (20 mM Tris–HCl, pH 8.0, 200 mM NaCl, 1% Triton X-100). Precipitated proteins were eluted from protein A sepharose by incubating with 20 μl of 0.1 M Glycine (pH 2.3) for 10 min at room temperature. SDS gel loading buffer was added to the resulting supernatants, which were then analyzed by immunoblotting for Mdm2.

2.5. Electrophoretic mobility shift assay (EMSA)

Nuclear extracts were prepared from AJ02-NM_0 cells as described above. A double-stranded p53 DNA oligonucleotide (Santa Cruz Biotechnology) was end-labeled with [γ-^{32}P] ATP (3000 Ci/mmol) using T4 polynucleotide kinase. Prior to the binding reaction, 5 μg of nuclear extract and 1 μl of Ab-1 p53 mouse monoclonal antibody (Oncogene Research Products) were mixed and incubated on ice for 20 min. Binding reactions were performed by mixing nuclear extract (in 7.5 μl) with 6.5 μl of 2.5 μg poly(dI·dC) and 1 μg BSA. After a 15-min incubation on ice, 40 fmol of labeled oligonucleotide (1 μl) was added to each reaction. Reactions were transferred to room temperature for an additional 15 min and then separated on a 4% polyacrylamide/Tris-borate EDTA gel.

2.6. Total RNA isolation and RNase protection assay

Total RNA was prepared from AJ02-NM_0 cells, tumor tissues and colon epithelial tissues using Trizol reagent (Invitrogen, Carlsbad, CA). Tissue samples were homogenized in Trizol using a mechanical homogenizer. mRNA levels were quantified using the RiboQuant multiprobe RNase protection assay system (Pharmingen, San Diego, CA). To probe p21, PERP, Bax, and Mdm2 expression levels, cDNA fragments (150–355 bp) were cloned into the pGEM-T Easy vector (Promega, Madison, WI). cDNA fragments of HPRT and GAPDH were also cloned to serve as internal controls. The cRNA probes from these templates were transcribed using reagents from Pharmingen. Isolated RNA (5 μg) was incubated with the labeled probes overnight at 56 °C and then digested with RNase. Protected RNA fragments were resolved on 5% sequencing gel. Image densitometry was performed using NIH Image.

2.7. Flow cytometric analysis of cell cycle and apoptosis

Following the various treatments, non-adherent and adherent cells were harvested for flow cytometric analysis. Adherent cells were detached from tissue culture plates using trypsin/EDTA solution, combined with non-adherent cells, gently resuspended and fixed in 500 μl ice-cold 70% ethanol at 4 °C overnight. After the fixation, cells were incubated at 37 °C for 30 min in PBS with 0.1% Triton X-100, 200 μg/ml RNAse A and 20 μg/ml propidium iodide. Samples were analyzed by flow cytometry using a FACScalibur machine (Becton Dickinson).

2.8. Two-dimensional gel electrophoresis

One hundred micrograms of nuclear extract from control or treated cells was concentrated and desalted by TCA precipitation. Samples were then resuspended in 170 μl of isoelectric focusing (IEF) sample buffer (8 M urea, 2% CHAPS, 50 mM DTT and 0.2% ampholytes pH 3–10 (Biorad, Hercules, CA). IEF was performed using the PROTEAN IEF system (Biorad) and 7 cm isoelectric strip gels pH 5–8. The isoelectric gels were passively rehydrated with the sample for 18 h prior to focusing for 15,000 V h. After IEF, gel strips were incubated for 15 min in equilibration buffer I (6 M urea, 2% SDS, 0.375 M Tris (pH 8.8), 20% glycerol, 2% DTT) and 15 min in equilibration buffer II (6 M urea, 2% SDS, 0.375 M Tris (pH 8.8), 20% glycerol, 2.5% iodoacetamide) prior to separation by SDS-PAGE.

2.9. Generation and transfection of p19/ARF siRNA and expression vectors

The siRNA sequence employed to suppress p19/ARF mRNA was: anti-sense 5′-aatcctggaccaggtgatgat-3′ and sense 5′-aaatcatcacctggtccagga-3′. This sequence was determined using the siRNA design support system (Takara Bio, Japan) and the siRNA duplex was synthesized using the Silencer siRNA construction kit (Ambion, Austin, TX). A non-targeting siRNA (Dharmacon, Lafayette, CO) was used in control reactions. siRNA was transfected by using Oligofectamine reagent (Invitrogen) and cells were analyzed 48–72 h after the transfection. The CMV-regulated p19/ARF cDNA was obtained in a pCMV-SPORT6 vector from Open Biosystems (Huntsville, AL) and transfected into cells with the Lipofecatmine 2000 reagent (Invitrogen).

2.10. Isolation and treatment of primary tumor tissue

Five- to 6-week-old male A/J mice were purchased from the Jackson Laboratories (Bar Harbor, ME). Mice were injected intraperitoneally once a week for 6 weeks with 10 mg/kg azoxymethane (AOM). Mice were sacrificed 24 weeks after the last injection of AOM. Immediately after sacrifice, the colons were rinsed with ice-cold PBS to remove fecal material, opened longitudinally and laid flat on a sheet of filter paper. Each tumor was excised from the surrounding tissue and cut into two halves, which were incubated in the culture medium with 40 μM Nutlin-3 or with vehicle control (DMSO) for 6 h at 37 °C. The medium used for these experiments was identical to that used for AJ02-NM_0 cell culture experiments, with the addition of gentamicin. Adjacent colon epithelial tissues that lacked visible tumors were also isolated and incubated in the same manner as tumor samples. One set of the samples was immediately frozen in liquid nitrogen and total cellular RNA was isolated for an RNase protection assay (RPA).

2.11. In situ apoptosis detection

Sections of colon tumor and adjacent normal epithelia from mice were fixed in 10% neutral buffered formalin, and

embedded in paraffin. Serial sections were analyzed by the TUNEL method using Apoptag Peroxidase In Situ Apoptosis Detection kit (S7100; Chemicon International, Temecula, CA) following the manufacturer's instructions. Briefly, 5-μm sections were deparaffinized, rehydrated and treated with 20 μg/ml proteinase K for 15 min at room temperature. Endogenous peroxidases were blocked by treatment with 3% H_2O_2. Doxigenin-conjugated nucleotides were placed directly onto the sections in the presence of the terminal deoxynucleotidyl transferase enzyme in a humidified chamber at 37 °C for 1 h. Sections were then incubated with an anti-digoxigenin antibody conjugate for 30 min at room temperature. Sections were washed in four changes of PBS, stained with 1.0% (w/v) methyl green counterstain, and evaluated with a light microscope. Images were captured and apoptotic bodies per field were counted and scored as a fraction of total epithelial cells.

2.12. Statistical tests

A one-tailed Student's *t*-test was employed to test the significance of differences between two groups. For the comparison of multiple groups against a single control, one-way ANOVA with Tukey–Kramer post hoc analysis was performed. A *p*-value of less than 0.05 was considered significant.

3. Results

3.1. Localization of p53, Mdm2 and p19/ARF in mouse colon cancer cells

AOM-induced colon tumors have an interesting phenotype in that a sequence-normal p53 protein is expressed, but is inactive for DNA binding and gene activation [18]. To better understand p53 regulation in these tumors, a cell line was generated from an AOM-induced colon tumor (AJ02-NM_0 cells) [20]. We first determined the cellular localization of two important p53 regulatory proteins in AJ02-NM_0 cells: p19/ARF and Mdm2. As shown in Fig. 1A, p53 was found in a high-salt nuclear extract of these cells. Mdm2 was also found in the high salt nuclear extract, as well as the cytosol, and the p53-activating p19/ARF protein was found within the nuclear matrix fraction (which included the nucleolar protein nucleolin). Localization of these proteins by immunofluorescence supported the observations of the cell fractionation experiment (Fig. 1B).

The co-fractionation of p53 and Mdm2 in the nuclear extract suggested that these proteins may be interacting. To determine if this was the case, an immunoprecipitation experiment was performed. As shown in Fig. 1C, a p53 antibody was able to precipitate Mdm2 from the nuclear extract. This result indicates that Mdm2 forms a complex with p53 in the nucleus of AJ02-NM_0 cells.

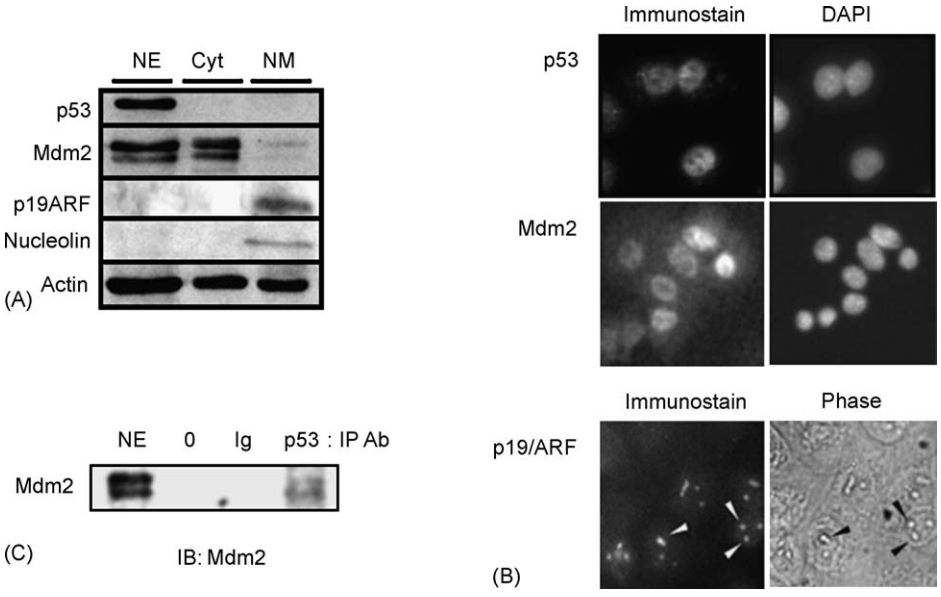

Fig. 1 – (A) Cellular fractionation analysis of p53, Mdm2 and p19/ARF. AJ02-NM_0 cells were fractionated into a cytosolic fraction (Cyt), a high-salt nuclear extract (NE) and a nucleolar/nuclear matrix fraction (NM). Each fraction was analyzed by immunoblotting for the indicated proteins. Nucleolin was used as a nucleolar marker. (B) Immunocytochemical analysis of p53, Mdm2 and p19/ARF in AJ02-NM_0 cells. Cells were stained with the indicated antibodies, which were detected by indirect immunofluorescence. The left panel images are the immunofluorscent images and the right panel images show nuclear DAPI staining (for p53 and Mdm2) or the phase image (for p19/ARF). (C) Interaction between Mdm2 and p53 in nuclear extracts from AJ02-NM_0 cells, as demonstrated by co-immunoprecipitation. Nuclear extracts were incubated with no antibody ("0" lane), normal serum ("Ig" lane) or a p53 antibody ("p53" lane). An immunoprecipitation was then performed using protein A sepharose beads. The resulting precipitate was then analyzed by immunoblotting with an antibody to Mdm2. An aliquot of nuclear extract prior to immunoprecipitation was also run on the gel to indicate the position of Mdm2 (the "NE" lane).

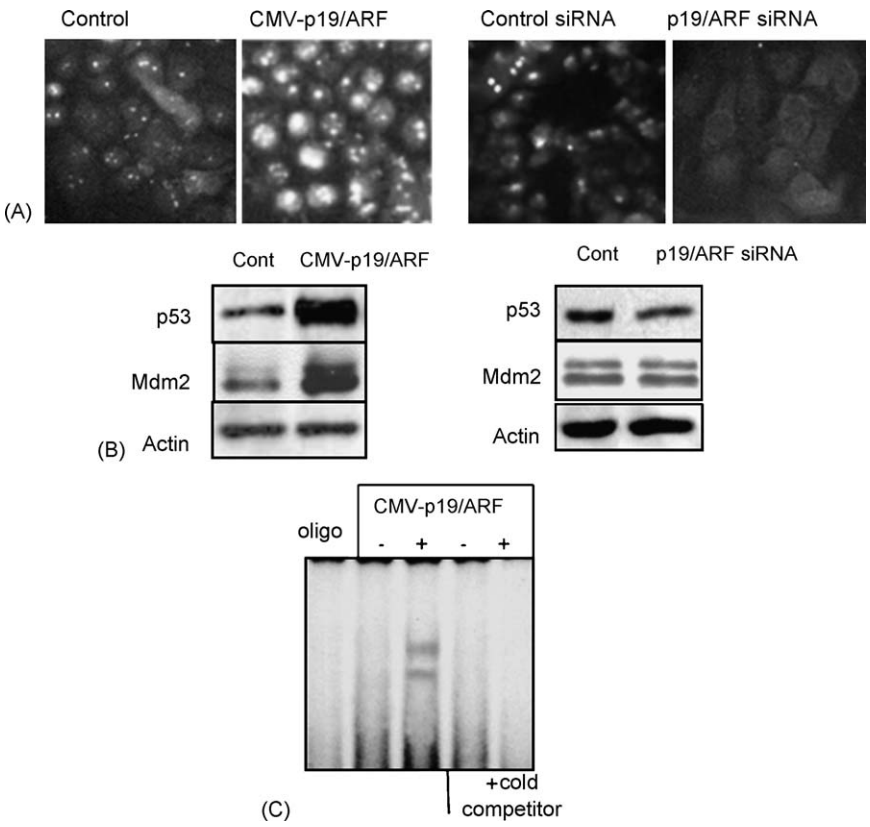

Fig. 2 – (A) Altering p19/ARF expression levels in AJ02-NM$_0$ cells. Cells were transfected with an empty CMV vector (control), a CMV-regulated p19/ARF expression vector (CMV-p19/ARF), a negative control siRNA (control siRNA) or a siRNA targeting p19/ARF (p19/ARF siRNA). Forty-eight hours after transfection, cells were analyzed for p19/ARF expression by immunocytochemistry. (B) Impact of p19/ARF expression levels on p53 expression. Cells were transfected with the p19/ARF expression vector or siRNA, as in (A), and were then analyzed for p53 and Mdm2 expression by immunoblotting. The blot was reprobed with actin, which served as a loading control. (C) Increased p19/ARF expression stimulates p53 DNA binding. AJ02-NM$_0$ cells were transfected with CMV-p19/ARF expression vector (lanes marked "+"), or an empty control expression vector (lanes marked "−"). Forty-eight hours after transfection, nuclear extracts were prepared from cells and tested for p53 DNA binding activity by the supershift reaction. The p53-DNA complex formed in p19/ARF over-expressing cells was inhibited by competition with a 50-fold molar excess of the unlabeled p53-binding oligonucleotide (lanes marked cold competitor). The first lane of the gel labeled "oligo" was the labeled oligonucleotide in the absence of nuclear extract.

p19/ARF has been shown to activate p53 by neutralizing the actions of Mdm2 [14,16,17]. The identification of Mdm2-p53 complexes in the nuclear fraction suggested that p19/ARF expression levels may not be sufficient to completely neutralize Mdm2. We therefore determined how altering p19/ARF expression influenced p53. As shown in Fig. 2, transfection of AJ02-NM$_0$ cells with a CMV-regulated p19/ARF gene increased both p19/ARF (Fig. 2A) and p53 expression levels (Fig. 2B). Increased p19/ARF expression also increased p53 DNA binding activity (Fig. 2C) and the expression of the p53-target gene Mdm2 (Fig. 2B). The converse experiment was also performed, in which AJ02-NM$_0$ cells were transfected with p19/ARF siRNA. This siRNA reduced the expression of p19/ARF (Fig. 2A), but did not dramatically influence the expression of p53 or Mdm2 (Fig. 2B). These experiments indicate that p53 expression and activity in AOM-induced cancer cells are regulated primarily through the actions of Mdm2 and that p53 can be stimulated through increased expression of p19/ARF.

3.2. *p53 activation in AJ02-NM$_0$ cells*

To further examine p53 activation in AJ02-NM$_0$ cells, these cells were treated with doxorubicin and 5-FU. Doxorubicin and 5-FU caused a modest increase in p53 levels (Fig. 3A). As shown by EMSAs, the p53 DNA binding activity in AJ02-NM$_0$ cells was low, but could be increased by doxorubicin and 5-FU (Fig. 3B). Activation of p53 by these agents was not accompanied by changes in p19/ARF expression or cellular localization (data not shown). Since evidence pointed to Mdm2 playing an important role in p53 regulation in AJ02-NM$_0$ cells, we tested their response to a number of recently developed Mdm2 inhibitors, including the chalcone derivative *trans*-4-Iodo, 4-boranyl-chalcone identified by Holak and colleagues, and the imidazoline analogue Nutlin-3 recently described by Vassilev et al. [19,21]. Nutlin-3 was found to be particularly active in AJ02-NM$_0$ cells. As shown in Fig. 3C, Nutlin-3 increased p53 levels in AJ02-NM$_0$ cells and activated p53 DNA binding in these cells to a level comparable to that achieved by 5-FU

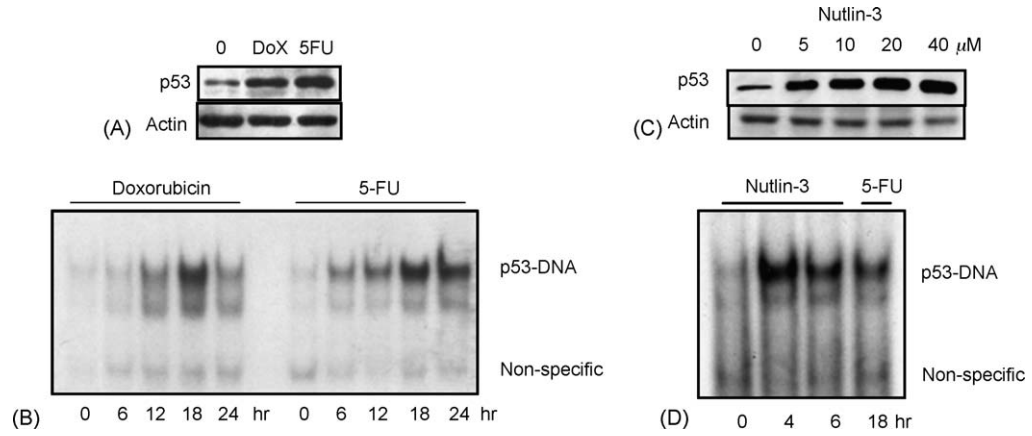

Fig. 3 – (A) Influence of chemotherapeutic agents on p53 protein levels. AJ02-NM$_0$ cells were treated with doxorubicin (Dox lane; 0.5 μM) or 5-FU (100 μM) for 18 h. Nuclear extracts were then analyzed for p53 and actin expression levels by immunoblotting. (B) Doxorubicin and 5-FU activate p53 DNA binding in AJ02-NM$_0$ cells. AJ02-NM$_0$ cells were treated with the indicated concentrations of doxorubicin or 5-FU for increasing lengths of time. Nuclear extracts were then prepared and tested for p53 DNA binding activity by an EMSA. The p53-DNA complex on the gel is indicated. (C) Influence of the Mdm2-inhibitor Nutlin-3 on p53 protein levels. AJ02-NM$_0$ cells were treated with the indicated concentration of Nutlin-3 for 18 h. Nuclear extracts were then analyzed for p53 and actin expression levels by immunoblotting. (D) Nutlin-3 activates p53 DNA binding in AJ02-NM$_0$ cells. AJ02-NM$_0$ cells were treated with Nutlin-3 (40 μM) or 5-FU (100 μM) for the indicated length of time. Nuclear extracts were then prepared and tested for p53 DNA binding activity by an EMSA. The p53-DNA complex on the gel is indicated.

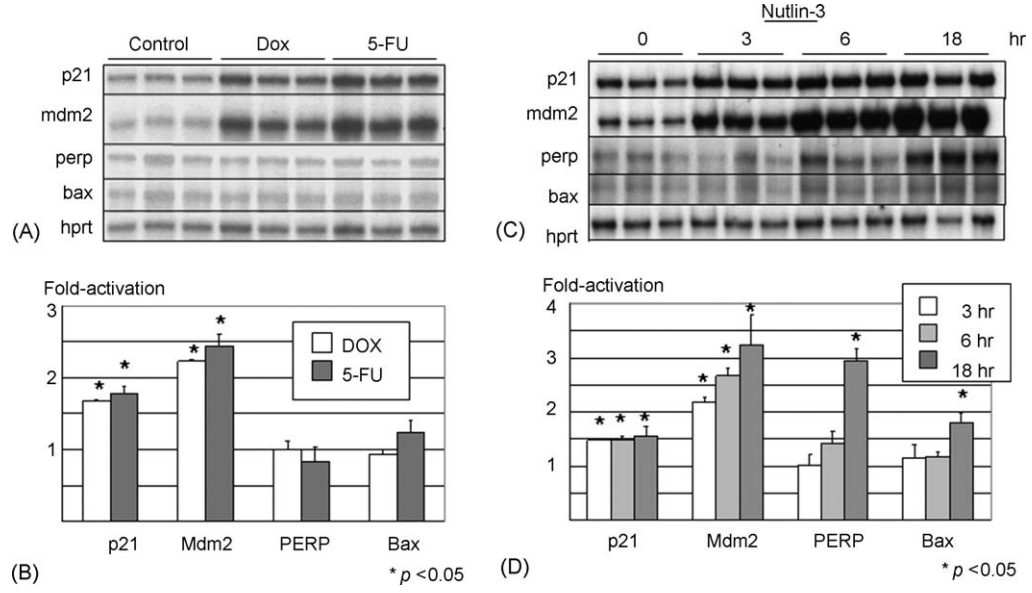

Fig. 4 – Activation of p53-target genes in AJ02-NM$_0$ cells. (A) AJ02-NM$_0$ cells were treated with doxorubicin (0.5 μM) or 5-FU (100 μM) for 18 h. RNA was then prepared from these cells and tested for expression of the p21, Mdm2, PERP and Bax by the RNase protection assay. HPRT mRNA serves as a loading control. The assay was performed in triplicate. (Different gel exposures are shown so that comparable signal intensities can be observed.) (B) Fold activation of p53 target genes after doxorubicin and 5-FU treatment. Signals from the protected RNA fragments in (A) were quantified by densitometry and normalized to HPRT. The fold activation was then calculated and plotted. Doxorubicin and 5-FU significantly increased the expression of p21 and Mdm2 ($^*p > 0.05$). (C) AJ02-NM$_0$ cells were treated with 40 μM Nutlin-3 (in triplicate) for the indicated lengths of time, after which RNA was isolated and analyzed by an RPA. The genes corresponding to the protected bands are listed at the left of the gel. (D) Fold-activation of p53 target genes after Nutlin-3 treatment. Signals from the protected RNA fragments in (C) were quantified by densitometry and normalized to the HPRT signal. The fold activation was calculated and plotted. Nutlin-3 significantly increased the expression of p21, Mdm2 PERP and Bax ($^*p > 0.05$).

(A)

	Cont (%)	Dox (%)	5-FU (%)
Sub-diploid	0.34	0.40	0.45
G0/G1	51.9	75.53	77.96
S	24.57	10.09	8.94
G2/M	22.62	13.55	12.30

(B)

	Cont (%)	Nutlin-3 (%)
Sub-diploid	1.74	0.54
G0/G1	61.92	57.03
S	11.18	6.89
G2/M	21.27	31.40

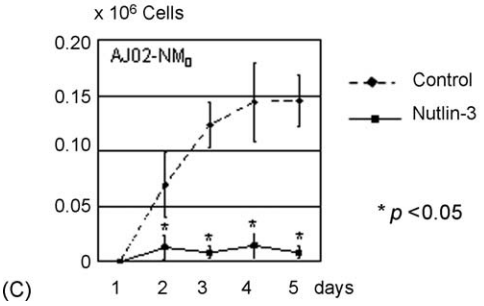

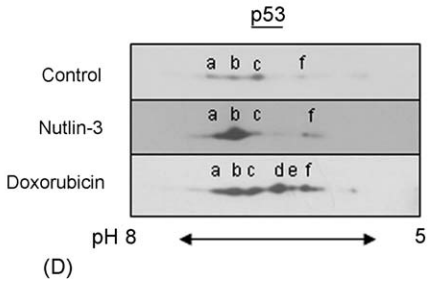

Fig. 5 – (A) Doxorubicin and 5-FU cause AJ02-NM$_0$ cells to arrest in G1 phase. Cells were treated with the indicated agent for approximately 24 h. Cells were then analyzed for DNA content by propidium iodide staining and flow cytometer analysis. The percentage of cells in G1, S and G2/M are indicated. Sub-diploid and potentially apoptotic cells were also quantified. (B) Nutlin-3 causes AJ02-NM$_0$ cells to arrest in G2/M phase. Cells were treated with the Nutlin-3 for approximately 24 h. Cells were then analyzed for DNA content by propidium iodide staining and flow cytometer analysis. The percentage of cells in G1, S and G2/M are indicated. Sub-diploid and potentially apoptotic cells were also quantified (but represented only a small fraction of the total cell population). (C) Nutlin-3 inhibits the proliferation of AJ02-NM$_0$ cells. AJ02-NM$_0$ cells were plated at a low density on a 24-well plate, and allowed to attach for 24 h. Nutlin-3 (40 μM) was then added to the culture medium, as indicated. Cells from triplicate cultures were then counted every 24 h. The growth inhibition by Nutlin-3 was significant at each time point analyzed ($^*p > 0.05$). (D) Doxorubicin treatment induces multiple modified forms of p53, whereas Nutlin-3 treatment does not. Nuclear extracts from control, Nutlin-3 treated or doxorubicin treated cells were subject to two-dimensional gel electrophoresis followed by p53 immunoblotting. The major forms of p53 are labeled "a" through "f" to facilitate comparison of the blots.

(Fig. 3D). p53 DNA binding was activated more rapidly by Nutlin-3 compared to 5-FU and doxorubicin, which likely reflects its more direct mechanism of action.

As shown in Fig. 4, doxorubicin, 5-FU and Nutlin-3 were all able to activate the expression of p53 target genes in AJ02-NM$_0$ cells. Specifically, all three agents were found to increase p21 and Mdm2 mRNA expression levels to a comparable extent. Nutlin-3 was, however, a better inducer of PERP and Bax expression (Fig. 4C and D). Cell cycle analysis was also performed on AJ02-NM$_0$ cells treated with these agents. As shown in Fig. 5A, doxorubicin and 5-FU triggered primarily a G1 arrest, whereas Nultin-3 induced the accumulation of cells in G2/M phase (Fig. 5B). The growth curves shown in Fig. 5C support the potent growth-suppressing actions of Nutlin-3 on AJ02-NM$_0$ cells. Similar results have been reported for p53-normal human colon cancer cells, such as HCT116 cells [22].

It has been previously reported that Nutlin-3 can activate p53 without causing a series of phosphorylation modifications induced by other p53 activators [22]. To compare the general influence of Nutlin-3 and doxorubicin on the p53 post-translational modification status, p53 was analyzed by two-dimensional gel electrophoresis. As shown in Fig. 5D, three forms of p53 were apparent in AJ02-NM$_0$ cells under normal culture conditions. Treatment of cells with Nultin-3 preferentially enhanced the expression level of one p53 isoform (labeled b). In contrast, treatment of cells with doxorubicin generated a more complex series of p53 modification states, with isoelectric point changes consistent with additional phosphorylation and/or acetylation modifications. These data indicate that Nutlin-3 generates a simpler collection of p53 modification states in AJ02-NM$_0$ cells. The differences in post-translational modification may contribute to the different cellular responses induced by Nutlin-3, such as Bax and PERP activation and G2/M arrest.

3.3. *Activation of p53 in primary colon tumors*

To gain further insight into the actions of Nutlin-3 on normal and neoplastic colon tissue, we incubated Nutlin-3 with tumor tissue and adjacent normal epithelium isolated from AOM-treated A/J mice and examined the expression of p53-regulated genes. As shown in Fig. 6, a 6-h incubation with Nutlin-3 significantly up-regulated the p53-target genes in tumor tissue. Interestingly, tumor tissue was less sensitive to Nutlin-3; although a modest increase was observed for some of the p53 target genes in the adjacent normal tissue, these increases did not achieve statistical significance. The activation of p53 in tumor tissue by Nutlin-3 was mirrored by an increase in the apoptotic index (Fig. 7). In contrast, normal adjacent tissue was largely intact following Nutlin-3 exposure. These findings further support Mdm2 as a potential target for chemotherapeutic agents against p53-normal colon tumors.

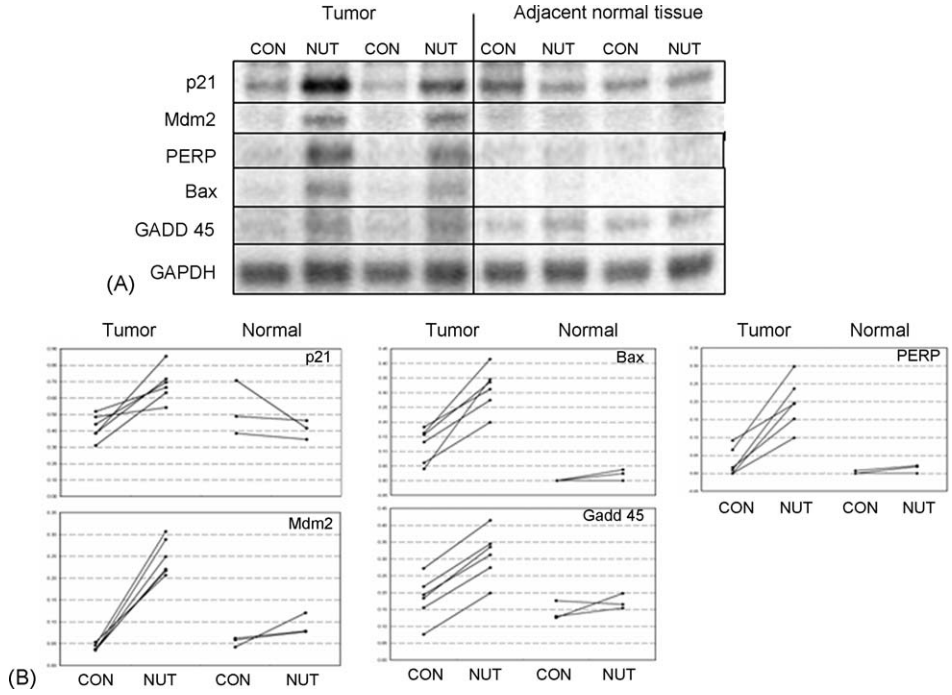

Fig. 6 – Activation of p53-target genes in AOM-induced mouse colon tumors. RNA levels of p21, Mdm2, PERP, Bax and Gadd 45 were compared between Nutlin-3 treated and non-treated tissue samples by the RNase protection assay. Two AOM-induced colon tumors and a portion of adjacent normal tissue were isolated from three animals. Each sample was cut into two halves, which were incubated for 6 h in the media with Nutlin-3 (40 μM) or with vehicle control (DMSO). GAPDH mRNA served as a loading control. (A) A representative autoradiogram of an RPA assay for p53-regulated genes. The results from Nutlin-3 treated and control RNA samples are shown side by side. (B) Quantified comparison between Nutlin-3 treated and control samples. Signals from the protected RNA fragments in (A) were quantified by densitometry and normalized to GAPDH. Data were analyzed by a One-way ANOVA followed by Tukey's multiple comparison test. The results of treated and non-treated samples from the same tissue are connected with a line. Nutlin-3 significantly increased the expression of p21, Mdm2, PERP, Bax and Gadd 45 ($p < 0.01$) in tumors.

4. Discussion

The p19/ARF-p53 oncogene checkpoint can effectively suppress carcinogenesis by triggering proliferation arrest and apoptosis of cells harboring an activated oncogene [23]. AOM-induced colon tumors in the mouse display an interesting phenotype with regard to this oncogene checkpoint in that tumors develop even though sequence normal p19/ARF and p53 proteins are expressed [18]. Here, we obtain evidence that AOM-induced colon cancer cells circumvent the p19/ARF-p53 oncogene checkpoint at least in part through the actions of the Mdm2 protein. Mdm2 in AOM-induced tumors suppresses p53 expression (to some extent) and effectively inhibits p53 DNA binding and transcriptional activation. Incomplete p53 degradation has been reported for cancer cells that over-express Mdm2 [24]. Possible explanations include insufficient expression of proteasome components, or altered expression of other auxiliary proteins, such as MdmX [25,26]. Regardless of the means of p53 inhibition by Mdm2, these actions are likely to be contributing to tumor cell growth in this model.

The actions of Mdm2 in AOM-induced tumor cells suggest that AOM-induced carcinogenesis bears some similarity to carcinogenesis driven by Mdm2 gene amplification. We recently reported that Mdm2 is expressed at elevated levels in AOM-induced tumors [18]. Increased Mdm2 expression in AOM-induced tumors is not the result of gene amplification, but instead appears to be the result of a selective transcriptional activation [27]. It is interesting to note that a polymorphism in the Mdm2 promoter that enhances SP1 binding and promoter activity has been linked to early cancer onset in humans, including the development of p53-normal colon cancers [28,29]. Excessive activation of Mdm2 expression in colonocytes may be a critical component of the AOM-induced carcinogenic pathway.

Many cancer therapies activate p53 by inducing the DNA damage response pathway, or some other stress-signaling pathway. Although these treatments can be effective, their genotoxic potential can lead to the development of secondary cancers, notably leukemias [30–32]. Mdm2 inhibitors represent a new class of cancer treatment agents that can activate p53 in cancer cells without triggering DNA damage [33,34]. A number of Mdm2 inhibitors have been developed, but there has been only limited testing of these compounds in cell culture and animal models. Our data indicate that Nutlin-3 is well-suited for mobilizing p53 in AOM-induced tumors and in p53-normal human colon cancer cells. In some regards, Nutlin-3 was found to be a better p53 inducer than doxorubicin and 5-FU; Nutlin-3 provided a more rapid induction of p53 DNA binding, and was able to activate a broader range of p53 target genes.

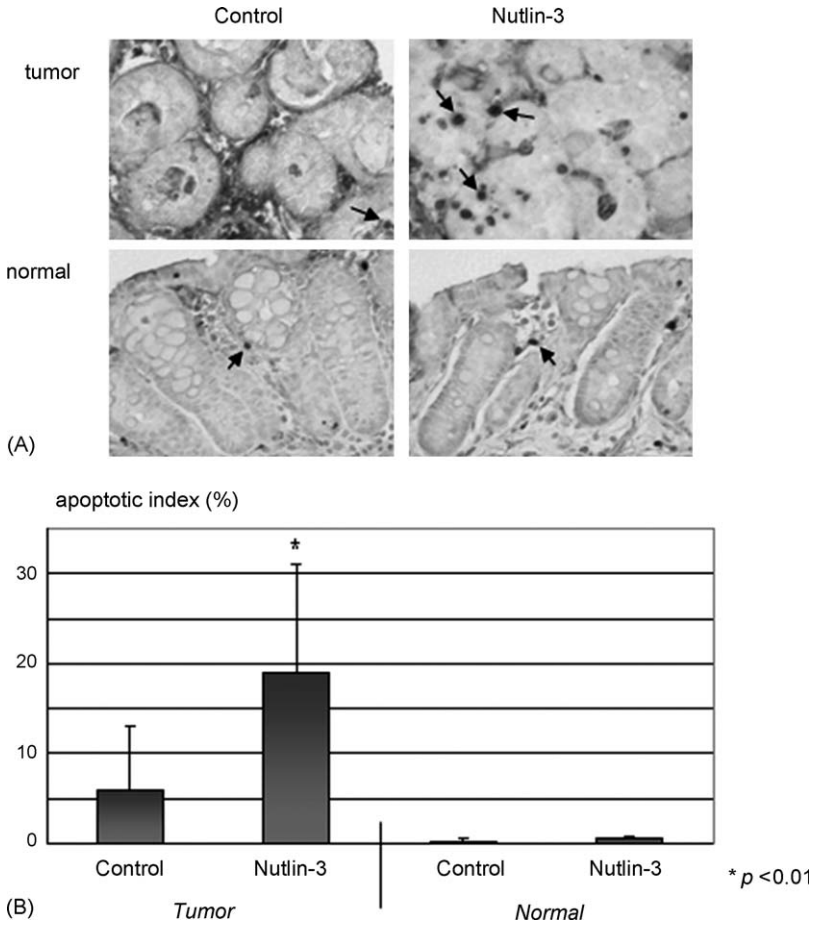

Fig. 7 – TUNEL analysis of apoptosis in colon tissues treated ex vivo with Nultin-3. Colon tissue was obtained from mice and treated with Nultin-3 (as described in Fig. 6). Tissue was then fomalin fixed and analyzed for the presence of apoptotic bodies by TUNEL staining. (A) Representative images of tissue sections processed by the TUNEL method. The arrows indicate examples of what were scored as apoptotic bodies. (B) The apoptotic index for normal and tumor tissue treated with or without Nutlin-3 was determined. Values were obtained from the analysis of eight tumors sections and four normal tissue sections.

These data suggest that Mdm2 inhibitors may not only provide for a more specific cellular response, but they may also be capable of inducing a more robust p53 response.

Mdm2 inhibition may be an effective means of treating p53-normal colon cancers, which constitute approximately 40% of all human colon cancers. Some p53-normal tumors also display elevated Mdm2 expression levels, which may represent a particularly responsive sub-group [35,36]. We found that p53 reactivation by Nutlin-3 ex vivo in colonic epithelium harboring tumors excised from carcinogen-exposed mice was more robust response than that observed in similarly treated normal adjacent mucosa. It is not clear what is responsible for the preferential activation of p53 observes in tumor tissue. It is possible that other p53-stimulating signals are active in the cancer tissue, which prime p53 for activation. These additional signals could be related to concomitant oncogene expression and/or increased levels of oxidative stress that have been associated with neoplastic tissues [37–41]. It is somewhat surprising that Mdm2 inhibitors can activate p53 at all, since p53 undergoes numerous post-translational modifications during a genotoxic stress response [22,42]. We have found that doxorubicin triggers extensive post-translational modification of p53 in AJ02-NM_0 cells, whereas the effects of Nutlin-3 on p53 modification are less dramatic. Differences in the post-translational modification status of p53 may lead to different cellular outcomes; whereas doxorubicin and 5-FU induce G1 arrest, Nutlin-3 causes cells to accumulate in G2/M.

Although there are a number of Mdm2 inhibitors presently available, it is not clear whether any of them will have suitable pharmacokinetic and pharmacodynamic properties for treating colon cancer. We have run a pilot experiment to determine whether an intraperitoneal injection of Nutlin-3 can activate p53 in AOM-induced colon tumors. Although a statistically significant activation of p21 was observed, the level of activation was not as dramatic as that observed following direct exposure of tumors ex vivo. In this regard, the AOM mouse model is well suited for determining how different delivery strategies might be exploited to target the Mdm2 inhibitor to colonic lesions (such as oral or rectal application routes). Our ex vivo data suggest that efficient delivery of an Mdm2 inhibitor to the colon may be a particularly effective means of targeting cancer cells while sparing normal tissue.

Acknowledgements

This work was supported by a National Cancer Institute grant to D.W.R. (CA-81428) and by the Neag Comprehensive Cancer Center.

REFERENCES

[1] Lozano G, Zambetti GP. What have animal models taught us about the p53 pathway? J Pathol 2005;205:206–20.
[2] Weber JD, Kuo ML, Bothner B, DiGiammarino EL, Kriwacki RW, Roussel MF, et al. Cooperative signals governing ARF-Mdm2 interaction and nucleolar localization of the complex. Mol Cell Biol 2000;20:2517–28.
[3] Tao W, Levine AJ. P19(ARF) stabilizes p53 by blocking nucleo-cytoplasmic shuttling of Mdm2. Proc Natl Acad Sci USA 1999;96:6937–41.
[4] Llanos S, Clark PA, Rowe J, Peters G. Stabilization of p53 by p14ARF without relocation of Mdm2 to the nucleolus. Nat Cell Biol 2001;3:445–52.
[5] Hasan MK, Yaguchi T, Sugihara T, Kumar PK, Taira K, Reddel RR, et al. CARF is a novel protein that cooperates with mouse p19ARF (human p14ARF) in activating p53. J Biol Chem 2002;277:37765–70.
[6] Moos PJ, Edes K, Cassidy P, Massuda E, Fitzpatrick FA. Electrophilic prostaglandins and lipid aldehydes repress redox-sensitive transcription factors p53 and hypoxia-inducible factor by impairing the selenoprotein thioredoxin reductase. J Biol Chem 2003;278:745–50.
[7] Moos PJ, Edes K, Fitzpatrick FA. Inactivation of wild-type p53 tumor suppressor by electrophilic prostaglandins. Proc Natl Acad Sci USA 2000;97:9215–20.
[8] Kastan MB, Zambetti GP. Parc-ing p53 in the cytoplasm. Cell 2003;112:1–2.
[9] Nikolaev AY, Li M, Puskas N, Qin J, Gu W. Parc: a cytoplasmic anchor for p53. Cell 2003;112:29–40.
[10] Nikolaev AY, Gu W. PARC: a potential target for cancer therapy. Cell Cycle 2003;2:169–71.
[11] Wadhwa R, Yaguchi T, Hasan MK, Mitsui Y, Reddel RR, Kaul SC. Hsp70 family member, mot-2/mthsp70/GRP75, binds to the cytoplasmic sequestration domain of the p53 protein. Exp Cell Res 2002;274:246–53.
[12] Kaul SC, Reddel RR, Mitsui Y, Wadhwa R. An N-terminal region of mot-2 binds to p53 in vitro. Neoplasia 2001;3:110–4.
[13] Wadhwa R, Takano S, Robert M, Yoshida A, Nomura H, Reddel RR, et al. Inactivation of tumor suppressor p53 by mot-2, a hsp70 family member. J Biol Chem 1998;273:29586–91.
[14] Iwakuma T, Lozano G. Mdm2, an introduction. Mol Cancer Res 2003;1:993–1000.
[15] Momand J, Jung D, Wilczynski S, Niland J. The Mdm2 gene amplification database. Nucleic Acids Res 1998;26:3453–9.
[16] Kobet E, Zeng X, Zhu Y, Keller D, Lu H. Mdm2 inhibits p300-mediated p53 acetylation and activation by forming a ternary complex with the two proteins. Proc Natl Acad Sci USA 2000;97:12547–52.
[17] Wadgaonkar R, Collins T. Murine double minute (Mdm2) blocks p53-coactivator interaction, a new mechanism for inhibition of p53-dependent gene expression. J Biol Chem 1999;274:13760–7.
[18] Nambiar PR, Giardina C, Guda K, Aizu W, Raja R, Rosenberg DW. Role of the alternating reading frame (P19)-p53 pathway in an in vivo murine colon tumor model. Cancer Res 2002;62:3667–74.
[19] Vassilev LT, Vu BT, Graves B, Carvajal D, Podlaski F, Filipovic Z, et al. In vivo activation of the p53 pathway by small-molecule antagonists of Mdm2. Science 2004;303:844–8.
[20] Belinsky GS, Claffey KP, Nambiar PR, Guda K, Rosenberg DW. Vascular endothelial growth factor and enhanced angiogenesis do not promote metastatic conversion of a newly established azoxymethane-induced colon cancer cell line. Mol Carcinog 2005.
[21] Stoll R, Renner C, Hansen S, Palme S, Klein C, Belling A, et al. Chalcone derivatives antagonize interactions between the human oncoprotein Mdm2 and p53. Biochemistry 2001;40:336–44.
[22] Thompson T, Tovar C, Yang H, Carvajal D, Vu BT, Xu Q, et al. Phosphorylation of p53 on key serines is dispensable for transcriptional activation and apoptosis. J Biol Chem 2004;279:53015–22.
[23] Serrano M. The INK4a/ARF locus in murine tumorigenesis. Carcinogenesis 2000;21:865–9.
[24] Knights CD, Liu Y, Appella E, Kulesz-Martin M. Defective p53 post-translational modification required for wild type p53 inactivation in malignant epithelial cells with Mdm2 gene amplification. J Biol Chem 2003;278:52890–900.
[25] Marine JC, Jochemsen AG. Mdmx as an essential regulator of p53 activity. Biochem Biophys Res Commun 2005;331:750–60.
[26] Jackson MW, Berberich SJ. MdmX protects p53 from Mdm2-mediated degradation. Mol Cell Biol 2000;20:1001–7.
[27] Guda K, Upender MB, Belinsky G, Flynn C, Nakanishi M, Marino JN, et al. Carcinogen-induced colon tumors in mice are chromosomally stable and are characterized by low-level microsatellite instability. Oncogene 2004;23:3813–21.
[28] Bond GL, Hu W, Bond EE, Robins H, Lutzker SG, Arva NC, et al. A single nucleotide polymorphism in the Mdm2 promoter attenuates the p53 tumor suppressor pathway and accelerates tumor formation in humans. Cell 2004;119:591–602.
[29] Menin C, Scaini MC, De Salvo GL, Biscuola M, Quaggio M, Esposito G, et al. Association between Mdm2-SNP309 and age at colorectal cancer diagnosis according to p53 mutation status. J Natl Cancer Inst 2006;98:285–8.
[30] Leone G, Voso MT, Sica S, Morosetti R, Pagano L. Therapy related leukemias: susceptibility, prevention and treatment. Leuk Lymphoma 2001;41:255–76.
[31] Smith MA, McCaffrey RP, Karp JE. The secondary leukemias: challenges and research directions. J Natl Cancer Inst 1996;88:407–18.
[32] Kubota M, Lin YW, Hamahata K, Sawada M, Koishi S, Hirota H, et al. Cancer chemotherapy and somatic cell mutation. Mutat Res 2000;470:93–102.
[33] Lain S, Lane D. Improving cancer therapy by non-genotoxic activation of p53. Eur J Cancer 2003;39:1053–60.
[34] Lane DP, Lain S. Therapeutic exploitation of the p53 pathway. Trends Mol Med 2002;8:S38–42.
[35] Tachibana M, Kawamata H, Fujimori T, Omotehara F, Horiuchi H, Ohkura Y, et al. Dysfunction of p53 pathway in human colorectal cancer: analysis of p53 gene mutation and the expression of the p53-associated factors p14ARF, p33ING1, p21WAF1 and Mdm2. Int J Oncol 2004;25:913–20.
[36] Hao XP, Gunther T, Roessner A, Price AB, Talbot IC. Expression of Mdm2 and p53 in epithelial neoplasms of the colorectum. Mol Pathol 1998;51:26–9.
[37] Skrzydlewska E, Stankiewicz A, Sulkowska M, Sulkowski S, Kasacka I. Antioxidant status and lipid peroxidation in colorectal cancer. J Toxicol Environ Health A 2001;64:213–22.
[38] Skrzydlewska E, Sulkowski S, Koda M, Zalewski B, Kanczuga-Koda L, Sulkowska M. Lipid peroxidation and antioxidant status in colorectal cancer. World J Gastroenterol 2005;11:403–6.

[39] Damalas A, Kahan S, Shtutman M, Ben-Ze'ev A, Oren M. Deregulated beta-catenin induces a p53- and ARF-dependent growth arrest and cooperates with Ras in transformation. EMBO J 2001;20: 4912–22.
[40] Sherr CJ, Weber JD. The ARF/p53 pathway. Curr Opin Genet Dev 2000;10:94–9.
[41] Groth A, Weber JD, Willumsen BM, Sherr CJ, Roussel MF. Oncogenic Ras induces p19ARF and growth arrest in mouse embryo fibroblasts lacking p21Cip1 and p27Kip1 without activating cyclin D-dependent kinases. J Biol Chem 2000;275:27473–80.
[42] Bode AM, Dong Z. Post-translational modification of p53 in tumorigenesis. Nat Rev Cancer 2004;4:793–805.